THE JOURNAL OF PHYSICAL CHEMISTRY C

Article

pubs.acs.org/JPCC

CO Adsorption on Reconstructed Ir(100) Surfaces from UHV to mbar Pressure: A LEED, TPD, and PM-IRAS Study

Kresimir Anic,[†] Andrey V. Bukhtiyarov,[†,‡] Hao Li,[†,§] Christoph Rameshan,*[,†] and Günther Rupprechter[†]

[†]Institute of Materials Chemistry, TU Wien, Getreidemarkt 9/BC, 1060 Vienna, Austria

[‡]Boreskov Institute of Catalysis SB RAS, Lavrentieva Ave., 5, Novosibirsk 630090, Russia

Supporting Information

ABSTRACT: Clean and stable surface modifications of an iridium (100) single crystal, i.e., the (1 × 1) phase, the (5 × 1) reconstruction, and the oxygen-terminated (2 × 1)-O surface, were prepared and characterized by low energy electron diffraction (LEED), temperature-programmed desorption (TPD), infrared reflection absorption spectroscopy (IRAS) and polarization modulation IRAS (PM-IRAS). The adsorption of CO in UHV and at elevated (mbar) pressure/temperature was followed both ex situ and in situ on all three surface modifications, with a focus on mbar pressures of CO. The Ir(1 × 1) surface exhibited c(4 × 2)/c(2 × 2) and c(6 × 2) CO structures under low pressure conditions, and remained stable up to 100 mbar and 700 K. For the (2 × 1)-O reconstruction CO adsorption induced a structural change from (2 × 1)-O to (1 × 1), as confirmed by LEED, TPD, and IR. For Ir (2 × 1)-O TPD indicated that CO reacted with surface oxygen forming CO_2. The (5 × 1) reconstruction featured a reversible and dynamic behavior upon CO adsorption, with a local lifting of the reconstruction to (1 × 1). After CO desorption, the (5 × 1) structure was restored. All three reconstructions exhibited CO adsorption with on-top geometry, as evidenced by IR. With increasing CO exposure the resonances shifted to higher wavenumber, due to adsorbate−adsorbate and adsorbate−substrate interactions. The largest wavenumber shift (from 2057 to 2100 cm^{-1}) was observed for Ir(5 × 1) upon CO dosing from 1 L to 100 mbar.

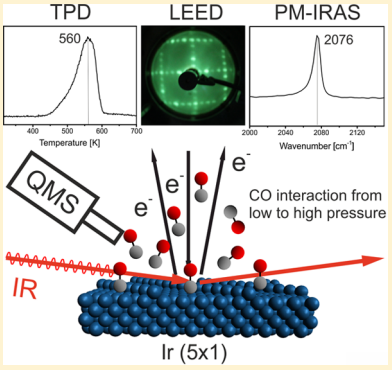

1. INTRODUCTION

Previous studies have shown that the Ir(100) surface exhibits interesting properties with respect to its surface reconstructions. Similar to other fcc metal surfaces (e.g., Au or Pt(100))[1] the Ir(100) surface undergoes a (1 × 1) → (5 × 1) surface reconstruction. According to experimental studies of the surface phonon distribution, as well as simplified pair potential modeling[2] and DFT studies[3] using periodic boundary conditions,[4] this behavior is caused by surface stress of the (1 × 1) surface, which can be reduced by surface structural changes. Hammer et al. reported that at temperatures above 180 K and in the presence of hydrogen the (5 × 1) reconstruction undergoes modification, with 20% of the surface atoms being expelled and forming ordered chains (rows) on the surface (see Figure 1).[5] Model studies of catalytic CO oxidation on surfaces of the Pt group metals revealed that some crystallographic orientations, particularly those prone to reconstructions, exhibit oscillatory behavior of the reaction rate.[6] This can be explained by the surface periodically switching from one reconstruction to another, depending on the type and coverage of the adsorbate (with concomitant changes of activity). Dispersed Ir on a TiO_2 support is a promising catalyst for low temperature CO oxidation as well as for the preferential oxidation of CO in the presence of hydrogen.[7] In the low pressure regime, the interaction with CO and the reactivity of different Ir surfaces has been examined by X-ray photoelectron spectroscopy (XPS), IRAS, ultraviolet photoelectron spectroscopy (UPS), high resolution electron energy loss spectroscopy (HREELS), and low energy electron diffraction (LEED).[8−12] Consequently, it seems worthwhile to examine the interaction of the different Ir surface terminations with mbar pressures of CO as well.

However, the (refractory) iridium surfaces have attracted interest not only due to their catalytic properties[13] but also for their use as substrate for growing graphene[14] or well-ordered oxide films.[15] In particular, Meyer et al.[15] reported the preparation of cobalt oxide (CoO and Co_3O_4) thin films by Co deposition on the Ir(100)-(1 × 1) surface under oxygen-rich conditions. Despite the (100) orientation of the substrate, the oxide films grow in a polar (111) orientation, which is difficult to obtain by other methods,[15] such as cleaving an oxide single crystal along the (111) plane or growing a single crystal of that orientation. The excellent properties of Ir(100) as support for well-ordered oxide films was another motivation for this detailed characterization. Since we intend to study the growth and catalytic properties[16] of epitaxially grown cobalt oxide model catalysts[15,17−19] (Co_3O_4 and CoO), detailed reference data (from UHV to elevated pressure) are required for the substrate, in order to confirm oxide film continuity, covering the entire substrate. In this respect, the properties of

Received: December 21, 2015
Revised: April 21, 2016
Published: April 21, 2016

DOI: 10.1021/acs.jpcc.5b12494
J. Phys. Chem. C 2016, 120, 10838−10848

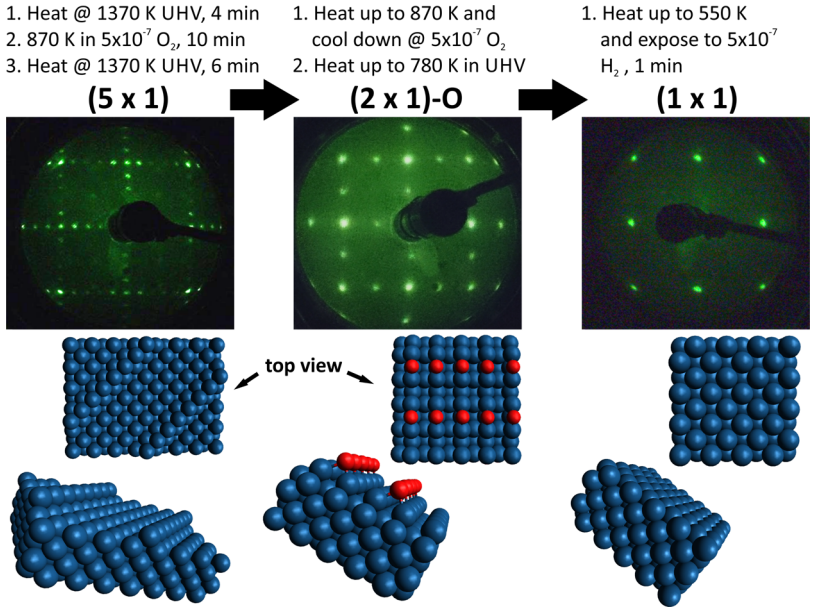

Figure 1. Preparation scheme (pressures in mbar), corresponding LEED patterns, and structural models of the (5 × 1) and (2 × 1)-O reconstructions and of the (1 × 1) surface. Electron energy for LEED was 80 eV.

the Ir(100) substrate at high CO pressures, which have not been studied up to now, are of great interest. Well-ordered cobalt oxide films are grown on the (1 × 1) surface reconstruction, but the (5 × 1) and (2 × 1)-O surfaces are needed for preparation of (1 × 1) and, accordingly, we focused our work on all three surface modifications. The experiments were mostly performed at 300 K as the growth of Co_3O_4 films (by deposition of cobalt in 5 × 10^{-6} mbar O_2 at 300 K) is performed at this temperature.

Clean and stable surfaces of the (1 × 1) orientation, the (5 × 1) reconstruction, and the oxygen terminated (2 × 1)-O surface were prepared as described below, with the surface structures (and changes thereof) being monitored by LEED. The adsorption of CO on the three reconstructions was followed by LEED, temperature-programmed desorption (TPD), infrared reflection absorption spectroscopy (IRAS), and polarization modulation (PM)-IRAS. The CO pressure was varied from UHV up to the mbar regime. For low pressure exposures only the on-top CO geometry was observed for all surfaces and coverages. The peak positions and shifts indicated a distinct dependence on pressure and temperature. Following CO exposure, TPD revealed the formation of CO_2 on the (2 × 1)-O surface, whereas the other two reconstructions both exhibited CO desorption around ∼465 and 565 K.

2. EXPERIMENTAL SECTION

All experiments were carried out in a custom-designed ultrahigh vacuum/high pressure cell system with a base pressure in the 5 × 10^{-10} mbar range, which has been described in detail elsewhere.[20−23] The preparation chamber is equipped with a differentially pumped quadrupole mass spectrometer (MKS eVison+), LEED optics (Specs ERLEED 1000-A), and a nonmonochromatic X-ray source (Specs XR 50, with AlKα and MgKα anode) combined with a Specs EA 150 PHOIBOS hemispherical analyzer. The UHV-compatible high pressure cell ("Rupprechter design")[22,23] is connected to a Fourier transform IR spectrometer (Bruker Vertex 60v) and a ZnSe photoelastic modulator operating at 34 kHz. The Ir(100) single crystal was purchased from MaTeck, mounted with tantalum wire on a coldfinger and heated resistively. For cleaning, the crystal was sputtered with 1 kV Ar^+ ions (p_{Ar} = 5 × 10^{-6} mbar, sputtering current = 2 μA) for 45 min followed by thermal annealing to 870 K. Crystal cleanliness was confirmed by XPS. The different surface reconstructions were prepared after sputtering in the following way: For preparation of the (5 × 1) surface the crystal was annealed to 1370 K for 4 min in UHV, followed by annealing in 5 × 10^{-7} mbar O_2 at 870 K for 10 min and a second annealing step in UHV (1370 K for 6 min).[24] In order to prepare the (2 × 1)-O surface, the freshly prepared (5 × 1) surface is heated to 870 K and cooled down in 5 × 10^{-7} mbar O_2 to RT and then again heated in UHV to 780 K. Starting from the (2 × 1)-O surface, the (1 × 1) surface can be prepared by heating the sample to 550 K and dosing 5 × 10^{-7} mbar H_2 for 1 min. This step differs only in the reducing gas from the preparation described in ref 25 for which CO was used instead of hydrogen in the final step. For the (2 × 1)-O surface the oxygen coverage is 1/2 with respect to the first atomic layer (missing row structure). With respect to the total surface area (from top view) the estimated O coverage is ∼1/6 ML.

Only high purity gases from Messer Austria were used for all experiments. The purity for oxygen and hydrogen was 5.0 (99.9990%) and the purity of CO was 4.7 (99.997%). Additionally, in order to avoid carbonyl contaminations a carbonyl absorber cartridge was installed in the CO gasline.[21] The cleanliness and chemical composition of the prepared samples were measured by XPS, and the surface structure was determined by LEED. Distinct LEED patterns of the different reconstructions were achieved using electron energies of 80 eV and are shown in Figure 1, along with structural models of the respective surfaces. For each of the (2 × 1)-O and the (5 × 1) surfaces, two rotational domains (90°) contribute to the respective LEED pattern. Due to the repeated work with H_2 and CO in the UHV system (and mbar CO in the high pressure cell), the base pressure increased to ∼1 × 10^{-9} mbar, consisting mainly of CO/H_2. This also likely led to the formation of the peculiar (5 × 1) reconstruction with an ordered row structure (see the detailed information and LEED I(V) measurements by

DOI: 10.1021/acs.jpcc.5b12494
J. Phys. Chem. C 2016, 120, 10838−10848

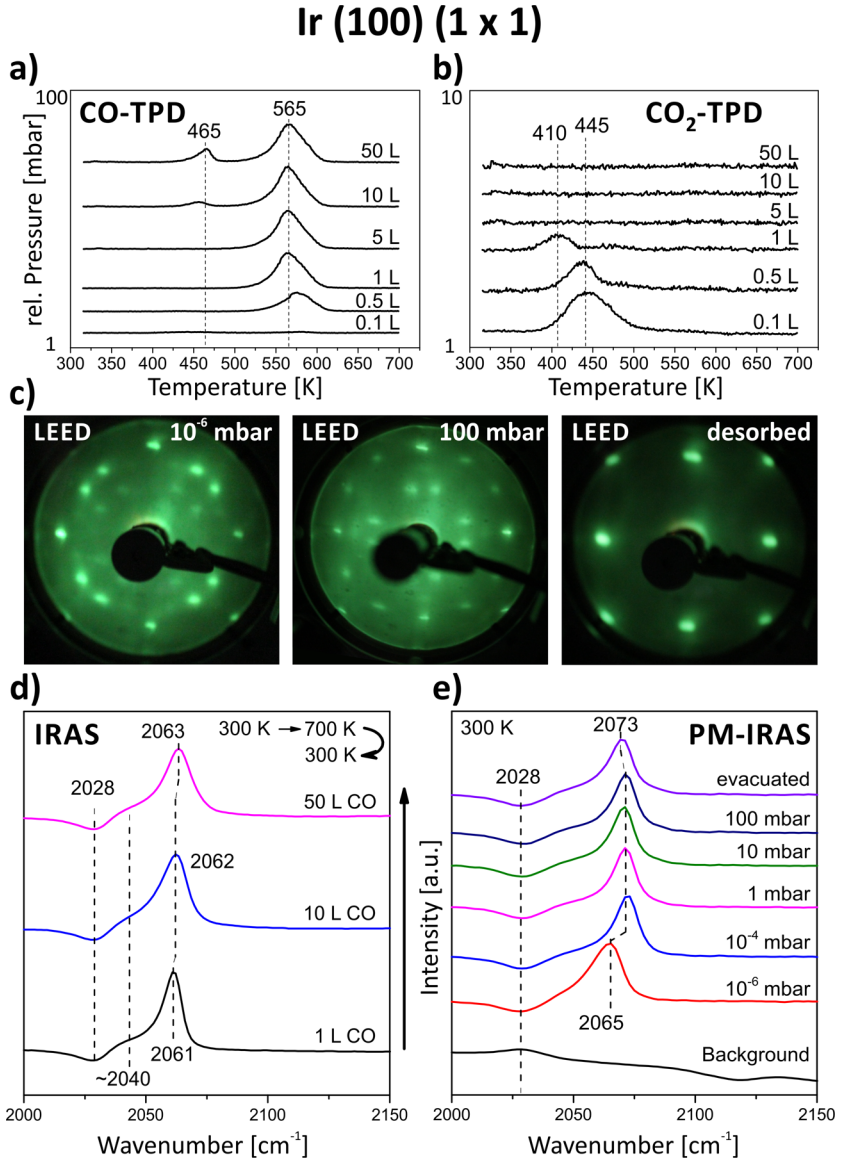

Figure 2. Summary of the experimental data of the Ir(100) 1 × 1 surface; (a,b) coverage dependent CO and CO_2 TPD series after the indicated CO exposure at RT, note the different scale for CO and CO_2 desorption; (c) LEED after exposure to10^{-6} mbar, 100 mbar CO, and after desorption, all acquired at RT. Electron energy was 80 eV; (d) IRAS spectra, each recorded before the respective TPD experiment, followed by re-exposure of CO at RT; (e) pressure-dependent PM-IRAS.

Hammer et al. in ref 5), as was confirmed by LEED. The (5 × 1) surface with hexagonally closed packed surface layer and the (5 × 1) surface with row structure exhibit the same diffraction pattern, but the two modifications have a different diffraction spot intensity distribution[5] (it cannot be excluded, though, that domains of the (5 × 1)hex structure were initially present on the surface).

Experiments in the low pressure range were performed both in the preparation and high pressure chamber. Dosing of O_2 and CO was carried out using a high precision leak valve. The Langmuir coverage was calculated assuming a sticking coefficient of unity. All IRAS measurements were done in the high pressure cell under UHV. The experiments in the high pressure range, extending up to 100 mbar, were carried out in the high pressure cell monitoring the pressure with a baratron gauge. All PM-IRAS measurements of CO adsorption (spectral range 1500 to 2600 cm^{-1}) utilized a modulation frequency of 34 kHz, with the data processing according to that described by P. Hollins.[26] After the mbar pressure exposure the high pressure cell was evacuated to UHV conditions, the sample was transferred back to the UHV chamber and TPD measurements were acquired in UHV.

3. RESULTS AND DISCUSSION

For all surfaces examined, their cleanliness was confirmed by XPS. In particular, C 1s spectra were acquired to exclude the presence of carbonaceous deposits before the adsorption experiments. Furthermore, XPS spectra taken after the adsorption experiments confirmed the absence of CO dissociation, i.e., only molecular CO was present during the experiments (see Supporting Information, Figures S1/S2). Also, the recombination of C and O would require much higher temperatures than those detected by TPD for CO desorption.

3.1. 1 × 1 Surface. Figure 2a,b shows TPD experiments carried out on the freshly prepared (1 × 1) surface. The first dose of 0.1 L CO was exposed to the pristine surface at 300 K,

DOI: 10.1021/acs.jpcc.5b12494
J. Phys. Chem. C 2016, 120, 10838−10848

for the following higher doses the "used" surfaces were cooled back to room temperature, CO was redosed, and the next TPD was acquired. The first CO-TPD spectrum did not exhibit CO desorption, but only CO_2 desorption (445 K), due to CO reaction with adsorbed oxygen to CO_2. Based on the preparation scheme, a small amount of surface O could not be avoided but readily reacted away upon the first three low CO doses (0.1, 0.5, 1 L). Most of the CO_2 was produced during the first TPD, however, pointing to ~0.1 ML of O on the surface. For CO exposures of 1, 5, 10, and 50 L, a growing CO desorption peak was observed at 565 K. The desorption energy, calculated by the Redhead equation using a pre-exponential factor of 10^{13} s^{-1}, was 141 kJ/mol for the 565 K desorption peak. Due to the rather broad desorption features, a variation in the desorption maximum of ±2 K would lead to a difference in desorption energy of ±0.5 kJ/mol. For 10 and 50 L exposures a second smaller desorption peak appeared at ~465 K, corresponding to a weaker bonded CO species with a desorption energy of 116 kJ/mol. The weaker bound species appeared after all sites for strongly bound CO was populated. In the course of the TPD experiment the weaker bound CO desorbed at ~100 K lower temperature, giving the remaining strongly bound CO room to relax in its ordered surface structure. Therefore, the desorption maximum for the strongly bound CO species remained at 565 K although the exposure was increased.

Figure 2c shows the LEED pattern of an ordered adsorbate overlayer after CO exposure (saturation coverage, 10^{-6} mbar) characterized by the spots of the substrate material and the additional ordered spots around the 1/2, 1/2 position. This overlayer pattern can be assigned either to a c(2 × 2) adsorbate structure with spot splitting on a square fcc(100) surface or to a c(4 × 2) overlayer structure with systematic spot extinctions (see the detailed discussion in the Supporting Information). These overlayer structures both correspond to a saturation coverage of 3/4 monolayer. Reasons for the spot splitting may be the presence of antiphase domain boundaries and/or regularly spaced domains of the overlayer structure. Both CO overlayer structures were already reported earlier, the c(4 × 2) structure by VanHove[27] and the c(2 × 2) structure by Kisters et al.[10] A LEED pattern was also acquired after desorbing CO at 700 K to check for structural alterations in the course of the TPD experiments, but the original (1 × 1) surface was restored after desorption.

To learn more about the nature of the adsorbed CO species IRAS spectra were recorded before the respective TPD experiments, i.e., after CO exposure at 300 K. After dosing 1 L of CO, two on-top CO species were detected, a main absorption peak at 2061 cm^{-1} and a distinct shoulder at ~2040 cm^{-1}. The 2061 cm^{-1} species is likely on-top CO on "regular" terraces, whereas the ~2040 cm^{-1} shoulder indicates step sites. The dip in the spectra at 2028 cm^{-1} results from CO traces (from residual gas in UHV) adsorbed on the "clean" surface, as indicated by the background spectrum in Figure 2e. Indeed, the same 2028 cm^{-1} species was also observed by Martin et al. for a CO exposure of 0.02 L.[9] After heating to 700 K (alike TPD), 10 L of CO were redosed and another IRAS spectrum was taken, with the same procedure repeated for 50 L of CO. All three spectra were very similar, despite the differences seen in the corresponding TPD runs. For the 1 L exposure the oxygen traces (~0.1 ML) on the surface do not affect the infrared band position. For the next CO exposure (10 L) the surface had already been heated to 700 K and was therefore free from oxygen traces. Apparently, the 465 K species seen in TPD did not show up in IRAS (and also not in LEED) indicating that it was a weakly bonded, likely disordered species, that only appeared after the stronger bonded sites had been populated.

Typically, higher exposures lead to higher coverage and thus to a blue shift of the wavenumber. However, for the current case such a shift is very small (only 2 cm^{-1}), suggesting that the 0.75 ML saturation coverage is obtained for 1, 10, and 50 L doses.

To examine the effect of gas pressure, PM-IRAS spectra were taken at 300 K on a freshly prepared surface, in a CO (equilibrium) pressure from 10^{-6} to 100 mbar (Figure 2e). The spectra display again two species but also a pronounced shift from 2065 to 2073 cm^{-1} with increasing pressure, pointing to increasing coverage[28] (blue-shift due to reduced electronic backdonation). Also here it seems that the trace oxygen amounts on the surface have no substantial effect on the CO adsorption properties and the infrared band position. Interestingly, after evacuation the spectrum remained nearly the same, i.e., the high coverage structure was stable at 300 K (CO desorbs at 565 K; cf. Figure 2 c).

This could also be observed by LEED (Figure 2c) that was taken after 100 mbar gas exposure and evacuation, which showed, compared to the 10^{-6} mbar exposure, an altered pattern. The reason is either that the distance of the c(2 × 2) spot splitting increased due to the presence of compression structures (shorter distance between CO molecules), in line with the observed shift to higher wavenumbers in PM-IRAS (from 2065 to 2073 cm^{-1}) for the 100 mbar exposure (and which remained stable after evacuation). Alternatively, the surface now resembled a c(4 × 2) structure, with multiple CO molecules per unit cell.

The calculated desorption energies of CO are summarized in Table 1 (including also the two other reconstructions and desorption of CO_2 from the (2 × 1)-O surface; see below). Desorption energies were estimated from the experimental desorption maxima using the Redhead equation with a pre-exponential factor of 10^{13} s^{-1}.

Table 1. Summary of the Estimated Desorption Energies of CO and CO_2 on the Different Surface Reconstructions, Calculated Using the Redhead Equation; Exposure Was 50 L of CO at 300 K

reconstruction	CO desorption temperature [K]	CO desorption energy [kJ/mol]	CO_2 desorption temperature [K]	CO_2 desorption energy [kJ/mol]
1 × 1	565	141		
	465	116		
2 × 1-O	565	141	330	82.5
	465	116	430	108
5 × 1	565	141		
	445	111		

3.2. 2 × 1-O Surface. The TPD spectra of room temperature CO exposure on the (2 × 1)-O reconstruction are shown in Figure 3a,b, starting at low CO exposure (0.1 L). The experiments were performed as described before, by cooling after the respective TPD to room temperature (RT), re-exposure of the "used" surfaces to CO at RT, followed by the next TPD.

For the 0.1 L of CO dose no CO (or CO_2) desorption was observed, as CO did not adsorb at this low exposure on the

DOI: 10.1021/acs.jpcc.5b12494
J. Phys. Chem. C 2016, 120, 10838−10848

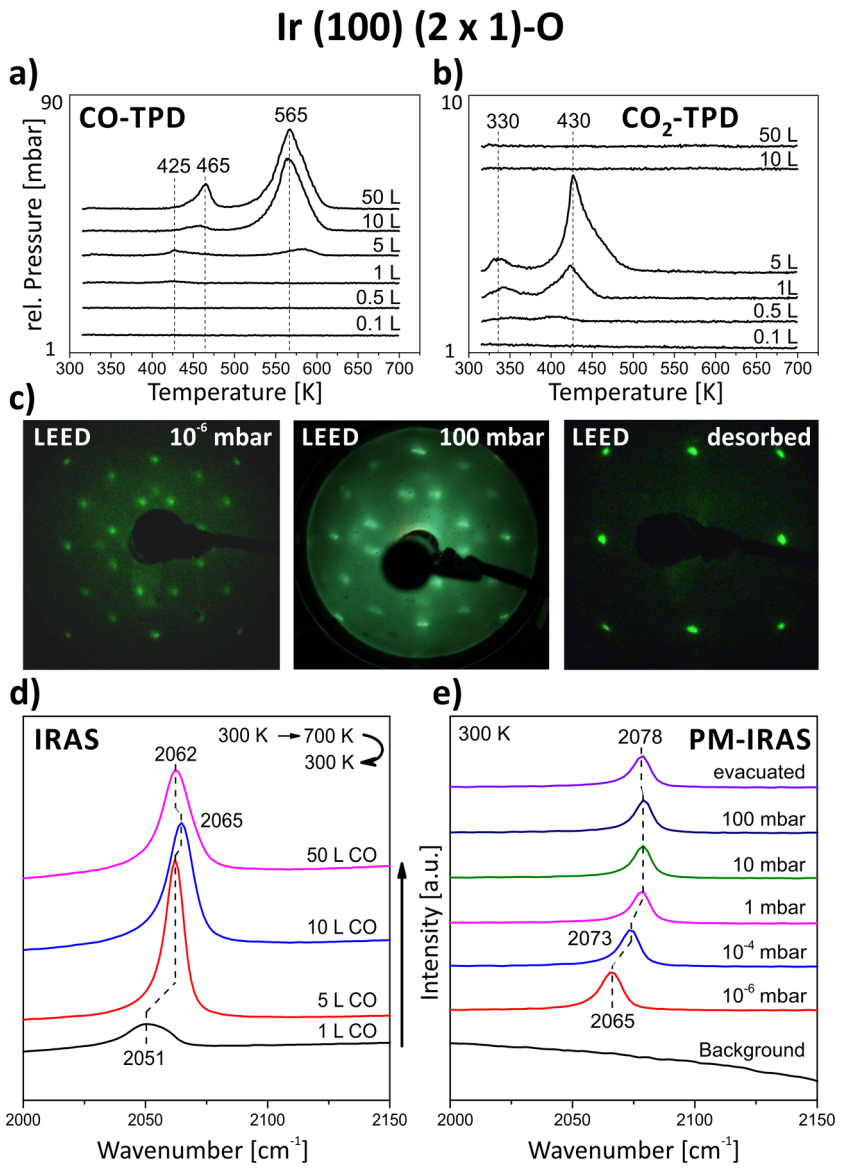

Figure 3. Summary of the experimental data of the Ir(100) 2 × 1-O reconstruction; (a,b) coverage-dependent CO and CO_2 TPD series after the indicated CO exposure at RT, note the different scale for CO and CO_2 desorption; (c) LEED after exposure to 10^{-6} and 100 mbar CO and after desorption, all acquired at RT. Electron energy was 80 eV; (d) IRAS spectra, each recorded before the respective TPD experiment, followed by re-exposure of CO at RT; (e) pressure-dependent PM-IRAS.

oxygen-terminated surface. As illustrated by the 3D model in Figure 1, the O-rows of the (2 × 1)-O reconstruction are preventing CO from adsorbing in the on-top geometry. Nevertheless, after the first TPD the surface is probably slightly altered and a small amount of CO can adsorb on the surface (defect sites) upon 0.5 L exposure. The adsorbed CO then reacts with O, leading to the small CO_2 peaks. Since some of the surface O has now been removed, more CO can adsorb upon 1 L dose, which subsequently reacts with surface O. This repeats for the 5 L exposure, creating strong CO_2 desorption signals and even small CO desorption peaks of unreacted CO. Both CO_2 desorption temperatures (330 and 430 K) are in line with those reported by King and co-workers for reaction of mixed oxygen and CO overlayers (p(2 × 1) and c(2 × 2) superposition) on Ir(100).[25] Apparently, at this state all surface O has been removed.

Upon 10 and 50 L of CO dosing at 300 K no CO_2 desorption peaks were observed anymore, but two CO peaks evolved, the main one at 565 K, and a smaller one at 465 K. Both CO peaks are identical to CO desorption from the (1 × 1) surface, indicating that during the sequential CO dosing the (2 × 1)-O reconstruction was successively lifted/reduced to the (1 × 1) surface. This is corroborated by XPS, which shows that the O 1s signal of surface oxygen had vanished after the TPD series (Supporting Information Figure S3).

The calculated desorption energies of CO on the (2 × 1)-O surface were 141 kJ/mol for the 565 K peak and 116 kJ/mol for the 465 K peak, again using the Redhead equation (it should be kept in mind that the surface is changing during the TPD experiment, and therefore, the calculation can only be an estimate).

The LEED pattern in Figure 3c, taken after exposure to 10^{-6} mbar CO (saturation coverage), again showed a similar ordered overlayer structure: a c(2 × 2) adsorbate structure with spot splitting or a c(4 × 2) adsorbate structure, as observed and discussed for the (1 × 1) surface. Upon 10^{-6} mbar CO

DOI: 10.1021/acs.jpcc.5b12494
J. Phys. Chem. C 2016, 120, 10838−10848

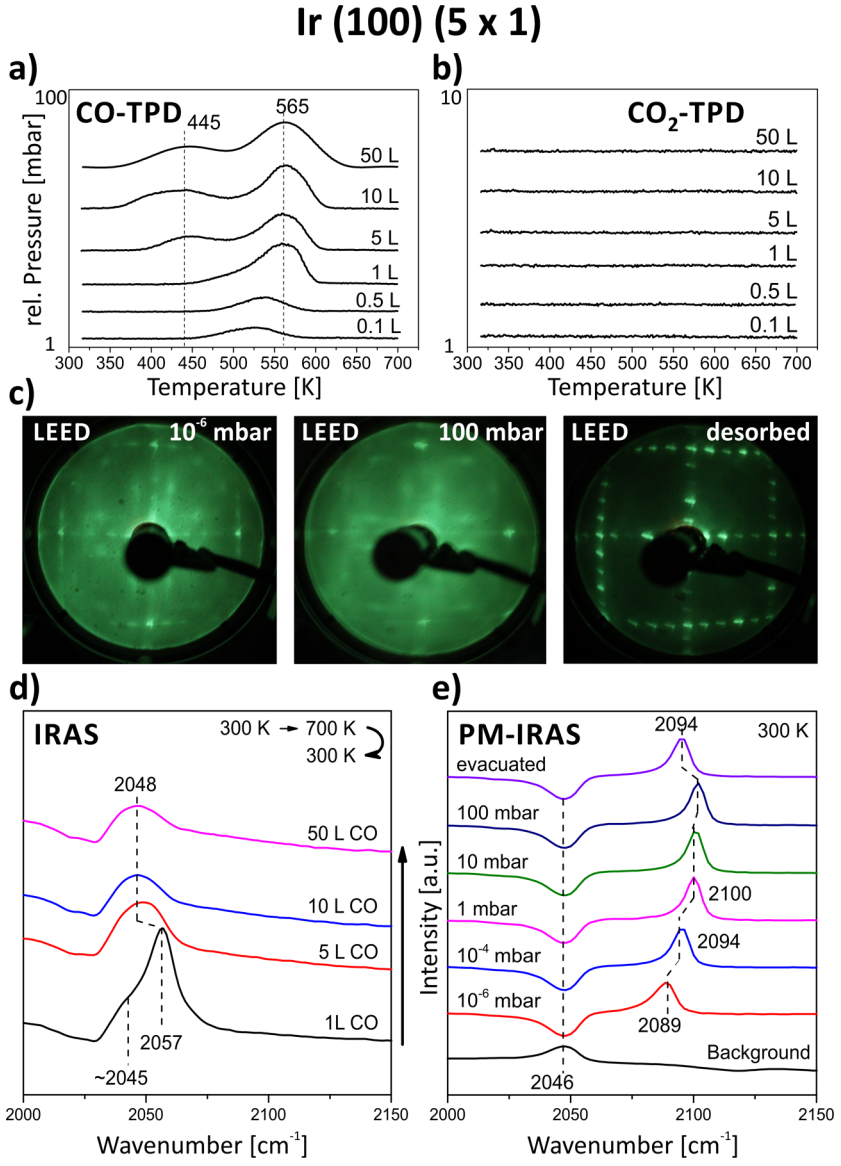

Figure 4. Summary of the experimental data of the Ir(100) 5 × 1 reconstruction; (a,b) coverage-dependent CO and CO_2 TPD series after the indicated CO exposure at RT, note the different scale for CO and CO_2 desorption; (c) LEED after exposure to 10^{-6} and 100 mbar CO and after desorption, all acquired at RT. Electron energy was 80 eV; (d) IRAS spectra, each recorded before the respective TPD experiment, followed by re-exposure of CO at RT; (e) pressure-dependent PM-IRAS.

exposure the (2 × 1)-O surface changed to the (1 × 1) surface, as the surface oxygen reacted subsequently with CO. This was supported by TPD, showing an onset temperature for CO_2 desorption already at ∼315 K. In the course of the repeated TPD experiments the (2 × 1)-O surface structure changed to a (1 × 1) surface, as also confirmed by LEED after CO desorption (heat to 700 K).

Adsorption on the Ir(2 × 1)-O reconstruction was studied for the first time by vibrational spectroscopy. Again, IRAS was applied to examine the adsorbed CO species at 300 K (Figure 3d), with the spectra recorded before TPD. After an exposure of 1 L to the (2 × 1)-O reconstruction only a weak and broad signal of adsorbed CO (2051 cm^{-1}) was observed since this surface is terminated by oxygen atoms that block CO adsorption. Upon heating to 700 K, the small amount of CO reacted with oxygen atoms to CO_2 (>315 K), which desorbed. Redosing 5 L of CO on the O-depleted surface then led to more CO adsorption and a stronger IRAS peak at 2062 cm^{-1}, which was the same as for CO adsorbed on the (1 × 1) surface in on-top geometry (again indicating a blue-shift due to higher CO coverage and resulting reduced electronic backdonation).

A dip in the spectra, induced by residual CO traces (cf. Figure 2d) is missing here, as the initially oxygen-terminated surface prevented CO adsorption and the background spectra were thus "CO-free". For 10 and 50 L exposure the vibrational frequency was 2065 and 2062 cm^{-1}, respectively. The intensity did not increase as the saturation coverage of 3/4 ML was already reached after 5 L exposure. Again this result indicates that the surface changes from (2 × 1)-O to (1 × 1) upon CO exposure.

On a freshly prepared (2 × 1)-O surface the pressure-dependent PM-IRAS spectra displayed only one on-top CO species at 300 K (Figure 3e). Upon exposing higher CO pressures to the (2 × 1)-O surface the C−O vibrational frequency increased from 2065 cm^{-1} (10^{-6} mbar) to 2073 cm^{-1} (10^{-4} mbar) and to 2078 cm^{-1} (1−100 mbar). This may be

DOI: 10.1021/acs.jpcc.5b12494
J. Phys. Chem. C 2016, 120, 10838−10848

due either once more to coverage-induced effects, i.e., reduced electronic backdonation from the metal to a single CO-π^* orbital,[29] and/or to structural changes of the surface from (2 × 1)-O to (1 × 1). Most likely both effects play a role. The structural change (O removal) of the surface might be somewhat slowed down because the sample was kept at 300 K during all PM-IRAS experiments. In comparison, during TPD experiments CO reacts with the surface oxygen at 330 K (and higher), but for PM-IRAS it is possible that at higher pressures CO reacts sequentially with the surface oxygen already at lower temperatures (the onset of the first CO_2 desorption feature in TPD is at ∼315 K). At low CO pressure the surface oxygen seems not to affect the infrared band positions and for higher CO pressures no oxygen is remaining on the surface. After evacuation CO remained adsorbed on the surface with the absorption band of 2078 cm^{-1} being characteristic of high coverage. This was also confirmed by LEED after 100 mbar CO exposure at 300 K, as can be seen by the overlayer structure in Figure 3c, which is identical to the corresponding structure on the (1 × 1) surface.

These experiments led to the conclusion that the (2 × 1)-O surface is not stable under reducing conditions and elevated temperatures, for the simple reason that the surface oxygen (that is stabilizing the structure) is consumed by CO.

3.3. 5 × 1 Surface. Figure 4a,b shows TPD experiments on a freshly prepared (5 × 1) surface carried out in the same manner as described for the other two surfaces. The coverage-dependent TPDs exclude CO_2 desorption for all exposures (i.e., the surface was O-free). At an initial dose of 0.1 L of CO, desorption set in at 530 K and shifted to 565 K upon exposures of 1 L and higher. This shift is most likely due to a change of the surface structure. After preparation, part of the surface may be (5 × 1)hex, which then changes to (5 × 1)row upon repeated CO exposure during the first two TPD runs. At exposures of 5 L and higher, a second fairly broad desorption peak was observed around 445 K (a small shoulder of the 565 K peak, corresponding to the 445 K desorption feature, could be already seen at 1 L exposure). The desorption peak maximum remained constant at higher CO exposures, but the peaks were broadened. Desorption energies were estimated by the Redhead equation and yielded a desorption energy of 141 kJ/mol for the 565 K peak and 111 kJ/mol for the 445 K peak.

The TPD profile can be explained in two ways: (i) originating from the specific row structure of the (5 × 1) reconstruction (with every fifth row sticking up) and, thus, by the different adsorption sites with different coordination numbers[30] (probable slightly stronger adsorption near the Ir rows) or, based on the similarity with the TPD profile in Figure 2a; (ii) originating from a local lifting of the reconstruction to a (1 × 1) reconstruction upon CO adsorption, as reported by Kisters et al.[10]

However, adsorbed CO was less ordered on the (5 × 1) surface. Upon exposure of 10^{-6} mbar CO (saturation coverage), LEED showed a rather complex, not well-ordered overlayer structure (Figure 4c). Beside very faint spots of the (5 × 1) reconstruction, spots of the (1 × 1) reconstruction were present. Additionally, faint rectangles of a CO overlayer structure could be observed. As shown in the next section these additional spots dynamically changed with adsorption temperature. The rather complex and faint LEED structure agrees with the observation of broad desorption peaks in TPD. Beside a local lifting of the (5 × 1) surface to (1 × 1), another reason for the not well-ordered LEED pattern may be related to the specific row structure that exhibits irregularities. In their detailed STM study, Hammer et al. showed that the distance between the rows can vary between three and seven atom rows (about 20−40% of the surface is affected, strongly depending on the exact preparation routine).[6] These irregularities of the surface affect the long-range order of adsorbed CO and thus the LEED pattern. After CO desorption during TPD, the (5 × 1) reconstruction was again visible in LEED (Figure 4c). This indicates that the local lifting of the surface to the (1 × 1) reconstruction occurred only when CO was present on the surface and that the surface locally switched back to the (5 × 1) reconstruction upon CO desorption.

IRAS was again applied to characterize the CO species adsorbed at 300 K (Figure 4d), with the spectra being recorded before the respective TPD experiments. After the first dose of 1 L of CO (before the first TPD) the (5 × 1) surface exhibited two on-top CO species at 2057 and ∼2045 cm^{-1}. The small spectral dip at ∼2030 cm^{-1} resulted from residual CO traces that were present when the background spectra were recorded. The two band positions are in line with results from Kisters et al.[10] and Martin et al.[9] for a similar CO exposure (1−1.5 L). The dip at ∼2030 cm^{-1} is comparable to the signal observed at 0.05 L exposure by Martin et al.,[9] again pointing to adsorption of small amounts of residual CO on the "clean" surface. Upon redosing CO following the first TPD, the 2057 cm^{-1} band decreased in intensity, whereas the signal at 2048 cm^{-1} increased. Similar to the observation by TPD, the repeated CO exposure/desorption during IRAS induced a change from the (partial) (5 × 1)hex to the (5 × 1)row structure, which is reflected by the difference of the 1 and 5 L IRAS spectra. Accordingly, the IR absorption bands for the 10 and 50 L CO exposures were then similar.

Due to the row structure of the surface there are two different adsorption sites for CO (see Figure 1): (i) a "regular" on-top position between the rows and (ii) an on-top position directly next to the rows at which CO additionally interacts with Ir atoms in the rows. Most likely, CO first populates the sites next to the rows (2057 cm^{-1}) and second the regular adsorption sites on the terraces (2048 cm^{-1}). This is also in line with TPD with the two CO desorption peaks at 445 and 565 K. The broad infrared signal also agrees with the observation of a disordered structure by LEED.

To examine the effect of higher gas pressure, PM-IRAS spectra were taken at 300 K in equilibrium CO pressure from 10^{-6} to 100 mbar (Figure 4e), using a freshly prepared surface. PM-IRAS experiments on the (5 × 1) reconstruction show one species of on-top CO. Again, a dip in the spectra (at 2046 cm^{-1}) originates from preadsorbed residual CO present in the background spectra, as discussed above. For 10^{-6} mbar CO the signal was at 2089 cm^{-1} and shifted at higher CO pressures to 2094 cm^{-1} (10^{-4} mbar) and 2100 cm^{-1} (1−100 mbar). The blue-shift of the IR signals can be explained by higher CO coverages and the resulting dipole−dipole coupling.[31] As there was no well-ordered CO overlayer structure we could not determine the saturation coverage via LEED patterns of the CO-(5 × 1) surface. After evacuation the infrared band shifted back to 2094 cm^{-1} indicating that the high pressure adsorption structure (in equilibrium CO) was not entirely stable in UHV. This was also confirmed by the faint LEED pattern after 100 mbar adsorption that was similar to the 10^{-6} mbar exposure pattern. Thus, it is likely that under higher equilibrium CO pressure a specific adsorbate structure was formed that has not yet been identified. This is supported by the relatively narrow

DOI: 10.1021/acs.jpcc.5b12494
J. Phys. Chem. C 2016, 120, 10838−10848

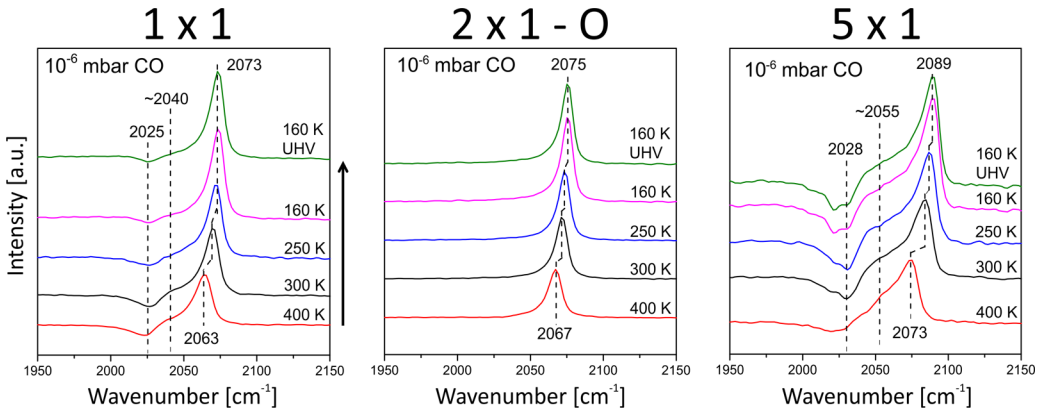

Figure 5. Temperature-dependent PM-IRAS for different Ir surfaces. Spectra were acquired in 1×10^{-6} mbar equilibrium CO, starting at 400 K. After cooling stepwise to 160 K in CO, the final spectrum was measured in UHV.

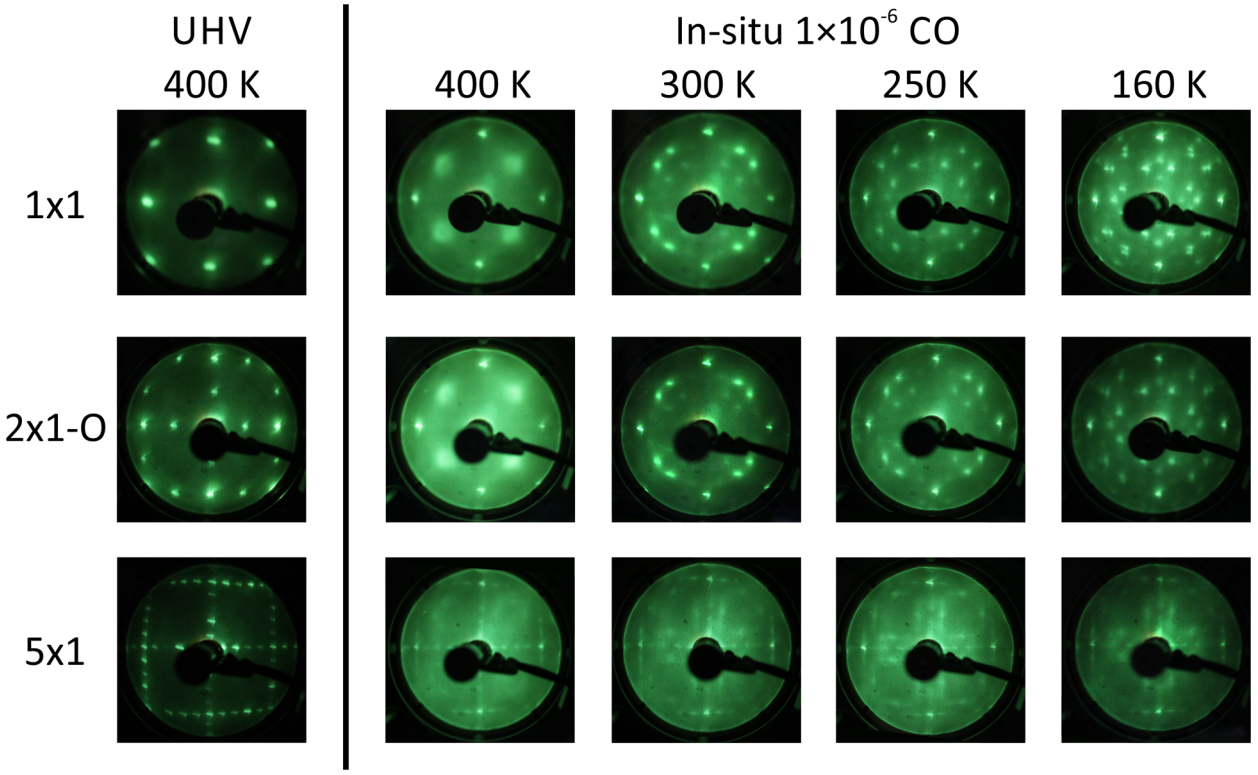

Figure 6. Summary of LEED patterns of the three pristine Ir(100) reconstructions in UHV and in situ LEED patterns in a 10^{-6} mbar CO environment at decreasing temperatures.

single on-top CO signal in PM-IRAS (as compared to the broad IRAS signal). However, based on TPD (Figure 4) the coverage seems to be even higher than that on Ir(1 × 1) (i.e., >0.75 ML).

3.4. Temperature-Dependent IR Studies. High CO coverage can either be obtained at higher temperatures by high gas pressure or, as an alternative, at low temperatures and low pressure. We have thus also performed experiments at 10^{-6} mbar CO, cooling the surfaces from 400 to 160 K.

For the temperature-dependent PM-IRAS measurements the surface was exposed to 1×10^{-6} mbar CO at 400 K. Then, the sample was cooled stepwise in CO to 160 K, and at the indicated temperatures PM-IRAS spectra were acquired. The last step was recording PM-IRAS at 160 K after evacuation. Background spectra were acquired for each surface and temperature prior to the respective experiment. At first we direct our attention to the (1 × 1) surface. Upon dosing 10^{-6} mbar CO at 400 K on the freshly prepared (1 × 1) surface (Figure 5), the PM-IRAS spectrum revealed two species of on-top CO, a main feature at 2063 cm^{-1} and a small shoulder at 2040 cm^{-1}. The dip (at 2025 cm^{-1}) of the IR intensity is again due to CO that is present in the background spectra of the "clean" surface. Upon cooling the sample the intensity was increasing due to higher CO coverage, and the main feature shifted to 2073 cm^{-1} accordingly. The shoulder stayed nearly constant at 2040 cm^{-1} during cooling. After evacuation the spectrum was identical to the spectrum in 10^{-6} mbar CO at 160 K, indicating that the adsorption structure was stable in UHV at this temperature (the maximum coverage at 160 K was 5/6 ML, as indicated by in situ LEED below).

For the (2 × 1)-O surface, the PM-IRAS spectra at 400 K in equilibrium CO pressure displayed only one on-top CO species

DOI: 10.1021/acs.jpcc.5b12494
J. Phys. Chem. C 2016, 120, 10838−10848

at 2067 cm^{-1}. As for the other infrared experiments on (2 × 1)-O the dip was again missing because the oxygen-terminated surface prevented CO adsorption while recording the background spectra. The wavenumber was very similar to that of the (1 × 1) surface. As already highlighted in Figure 3 (TPD), above 315 K the surface oxygen of this reconstruction reacts with CO to CO_2. Therefore, this surface had already changed to (1 × 1) in 1 × 10^{-6} mbar CO at 400 K. With decreasing temperature the signal was shifting to higher wavenumbers (2075 cm^{-1} at 160 K), which was again very similar to the (1 × 1) surface (2073 cm^{-1}). The signal at 160 K in CO and after evacuation was identical, indicating again that the CO surface structure was stable in UHV at 160 K.

For the (5 × 1) reconstruction PM-IRAS detected two distinct on-top CO species at 400 K (at 2073 cm^{-1} and a shoulder at ∼2055 cm^{-1}). They can again be explained by the specific row structure or the local lifting of the reconstruction to (1 × 1), as discussed in the previous section. The latter is supported by the LEED patterns after CO adsorption (Figures 4c and 6), in which a faint pattern of the (5 × 1) reconstruction and the reflexes of the (1 × 1) reconstruction can be observed. Also the shoulder in the infrared signal at ∼2040−2055 cm^{-1} was similar for (1 × 1) and (5 × 1). Upon cooling the surface in CO to lower temperatures, the main signal shifted to 2089 cm^{-1} and gained intensity due to higher CO coverage. The shoulder remained nearly constant. Due to the nonordered CO adsorption structure in LEED, an estimation of the coverage cannot be provided for Ir(5 × 1). However, based on TPD (Figure 4) the coverage seems to be even higher than that on Ir(1 × 1) (i.e., >0.75 ML). After evacuation no change in the spectrum was observed, i.e., this structure was stable at 160 K.

3.5. In Situ LEED Series. In this experiment the three different surfaces were kept in 10^{-6} mbar (equilibrium) CO pressure while acquiring LEED patterns. The starting temperature was 400 K, followed by stepwise cooling to 300, 250, and 160 K (Figure 6).

When the (1 × 1) and (2 × 1)-O surfaces were exposed to 1 × 10^{-6} mbar CO at 400 K, both LEED patterns were identical, showing large diffuse spots of a CO adsorption layer, beside the substrate spots. The diffuse clouds could represent a not well ordered c(2 × 2) overlayer structure with 0.5 ML coverage (at 400 K the adsorbed CO is rather mobile). Taking into account the IR and TPD data from previous sections, we conclude that the (2 × 1)-O structure changed to the (1 × 1) structure upon CO exposure at 400 K. Upon cooling to 300 K, the same ordered CO overlayer structure of c(2 × 2) with spot splitting started to evolve on both surfaces, which is in line with the c(2 × 2) adsorption reported by Titmuss et al.[32] The reason for the spot splitting are likely antiphase domain boundaries[33] and/or regularly spaced domain structures. At 250 K, it seems that the spot splitting increased and the spots became sharper. This may be due to the transition from a c(2 × 2) structure with spot splitting to a true c(4 × 2) structure (0.75 ML coverage; note that some diffraction spots of the latter are missing due to intensity reasons and/or destructive interference; see SI). At 160 K, the LEED patterns of Ir(1 × 1) and the former Ir(2 × 1)-O changed again and additional small spots could be observed between the main reflexes of the substrate. This indicates a further transition from c(4 × 2) to c(6 × 2) when the temperature is lowered and the coverage is increased to 5/6 ML. Again some diffraction spots (1/2, 1/2 positions) are missing due to systematic spot extinctions.

The (5 × 1) surface showed quite a different adsorption behavior. At 400 K, when the CO coverage was low, spots from the (5 × 1) reconstruction were still visible. When the temperature was reduced to 300 K and the CO coverage increased, the features from Ir(5 × 1) started to vanish. Instead, spots of the (1 × 1) surface and blurred rectangles of a CO overlayer structure appeared in LEED. As discussed before, the reason is related to the local lifting of the (5 × 1) reconstruction to (1 × 1) and irregularities of the row structure. At 250 and 160 K, the LEED was very similar, again with no well-ordered CO structure. The difference between 300, 250, and 160 K is that mainly the contributions of the three structures (spots from (5 × 1), spots from (1 × 1), and the blurred rectangles) were different. This indicates a rather dynamic and temperature-dependent behavior of the (5 × 1) surface during CO adsorption.

3.6. Comparison of the Three Surfaces. In the following, the most characteristic properties of the three reconstructions are compared. Upon CO adsorption, both the (1 × 1) and (2 × 1)-O surface initially showed CO_2 desorption in the TPD experiments, resulting from CO reaction with oxygen bound to the surface. In the case of Ir(1 × 1) oxygen traces result from the preparation routine (reduction of (2 × 1)-O in H_2 at 550 K) and the amount of CO_2 was thus small. For Ir(2 × 1)-O the surface is terminated by oxygen (Figure 1) that is successively reacting with adsorbed CO to CO_2 (during the repeated TPD runs). After all oxygen has been removed from the surface, the (1 × 1) and (2 × 1)-O surfaces exhibited very similar CO desorption features (main peak at 565 K and small peak at 465 K). As discussed, the reason is the change of the (2 × 1)-O surface to Ir(1 × 1) upon CO exposure and heating.

For Ir(5 × 1) the preparation routine yields an O-free surface, and thus, there was no CO_2 desorption after CO adsorption. For the (5 × 1) reconstruction the TPD spectra displayed broader signals at 565 and 445 K. For all terminations a first order desorption behavior was observed.[34]

For LEED, after room temperature CO adsorption at low and elevated pressure, both the (1 × 1) and (2 × 1)-O surface showed the same pattern of an ordered CO overlayer structure (which can be assigned either to c(2 × 2) with spot splitting or to c(4 × 2) with missing diffraction spots, both with 3/4 ML coverage, see also Supporting Information). After CO desorption both surfaces exhibit a (1 × 1) LEED pattern. As explained before, this is due to the change of the (2 × 1)-O surface to (1 × 1). For Ir(5 × 1), upon CO exposure no ordered overlayer structure but only a faint LEED pattern of multiple features (Figure 4) could be observed. Possible reasons, such as the local lifting to (1 × 1) and irregularities in the row structure were discussed in previous sections. After CO desorption the (5 × 1) surface was restored.

The first IRAS spectra of adsorbed CO (1 L) were collected prior to performing TPD. All other spectra at higher exposures were acquired after performing a TPD experiment. On Ir(1 × 1) a dip was observed, resulting from preadsorbed CO traces, probably located at defect sites. This was missing for Ir(2 × 1)-O, as the oxygen-terminated surface initially blocks CO adsorption. After the (2 × 1)-O surface had changed during TPD, the absorption infrared bands (∼2060 cm^{-1}) were very similar to those on Ir(1 × 1). The (5 × 1) surface showed a different behavior with the absorption bands being rather broad in IRAS (∼2048 cm^{-1}), which was in line with the observation of broad TPD signals and a nonordered adsorption structure in LEED.

DOI: 10.1021/acs.jpcc.5b12494
J. Phys. Chem. C 2016, 120, 10838−10848

For PM-IRAS in 10^{-6} mbar (equilibrium) CO pressure and at RT, on-top CO at 2065 cm^{-1} could be observed both for (1 × 1) and (2 × 1)-O (although the first additionally showed a small shoulder at 2050 cm^{-1}). With increasing CO pressure the band shifted to higher wavenumbers for both surfaces when the CO coverage increased; to 2073 cm^{-1} for Ir(1 × 1) and 2078 cm^{-1} for Ir(2 × 1)-O at 100 mbar. For (2 × 1)-O the initially present oxygen seemed not to affect the infrared band position. At higher CO pressures oxygen gradually reacted away as discussed before. Ir(5 × 1) exhibited one signal for on-top CO starting at slightly higher wavenumber (2089 cm^{-1}), which shifted to even higher wavenumbers (2100 cm^{-1}) at 1 mbar and above (likely due to coverage higher than on the other terminations). A similar behavior also occurred in temperature-dependent PM-IRAS. Upon cooling in CO, the (5 × 1) surface again showed the highest shift in wavenumber (2089 cm^{-1}), whereas for the (1 × 1) surface only a shift to 2073 cm^{-1} and for the (2 × 1)-O surface a shift to 2075 cm^{-1} could be observed at 160 K (due to reaction with O at 400 K, the (2 × 1)-O had turned to (1 × 1), though).

For temperature-dependent in situ LEED, the (1 × 1) and (2 × 1)-O surfaces show very similar LEED patterns (once more because the (2 × 1)-O surface converts to (1 × 1) at 400 K). At 400 K only large faint spots were observed for adsorbed CO. At 300 K an ordered overlayer structure of either c(2 × 2) with spot splitting or c(4 × 2), both with a coverage of 3/4 ML, could be observed. At 160 K, a further transition from c(4 × 2) to c(6 × 2) (coverage 5/6 ML) occurred. For the (5 × 1) surface no ordered CO overlayer was observed by in situ LEED in the entire temperature range.

4. CONCLUSIONS

The interaction of CO, from UHV to elevated pressure/temperature, with three different reconstructions of the Ir(100) surface was studied by LEED, TPD, and IRAS/PM-IRAS:

Ir(100)(1 × 1). LEED patterns showed that room temperature CO adsorption led to an ordered adsorbate overlayer structure, which can be assigned either to c(2 × 2) with spot splitting or to c(4 × 2), both with 3/4 ML coverage. Corresponding TPD experiments revealed distinct desorption features at 565 and 465 K (desorption energy 141 and 116 kJ/mol, respectively). Infrared experiments displayed two on-top CO signals (2061 and 2040 cm^{-1}). With increasing CO pressure a shift to 2073 cm^{-1} was observed (100 mbar CO). The same shift was observed in 1 × 10^{-6} mbar CO when coverage was increased by lowering the temperature from 400 to 160 K. This is in line with changes observed by LEED, indicating an even denser structure at 160 K. In summary, Ir(1 × 1) is stable, even for high pressure CO and high temperature.

Ir(100)(2 × 1)-O. On the pristine oxygen-terminated surface, CO adsorption was blocked at the lowest exposures. However, small amounts of CO could still adsorb (which then reacted with small amounts of O during TPD), and after repeated adsorption and continued reaction of surface O (and its removal as CO_2), the surface converted to (1 × 1). Higher CO doses (1 and 5 L) resulted in significant CO_2 desorption at 430 and 330 K (108 and 82.5 kJ/mol desorption energy, respectively). After full removal of surface oxygen, desorption features identical to those of Ir(1 × 1) were observed. Consequently, CO adsorption produced the same ordered adsorbate overlayer as on (1 × 1). Only one species of on-top CO was detected by IRAS and PM-IRAS (2051 and 2065 cm^{-1}, respectively, surface O still present). With increasing pressure, a shift to 2078 cm^{-1} was observed by PM-IRAS (100 mbar CO, no surface oxygen left). Post-reaction LEED indicated that the surface changed to Ir(1 × 1) after TPD and high pressure CO exposure. These results indicate that the (2 × 1)-O surface is not stable in reducing atmosphere and at elevated temperature, leading to a structural change to Ir(1 × 1).

Ir(100)(5 × 1). No ordered CO adsorption structure was observed by LEED. Corresponding TPD experiments showed broad CO desorption features with maxima at 565 and 445 K (desorption energy 141 and 111 kJ/mol, respectively). IRAS displayed two on-top CO signals at 2057 and ∼2045 cm^{-1} that turn into a fairly broad signal upon higher exposures. A shift to 2100 cm^{-1} was observed for 100 mbar CO by PM-IRAS. Similar wavenumber shifts were obtained in 1 × 10^{-6} mbar CO by increasing the coverage by lowering the sample temperature to 160 K (2089 cm^{-1}). At lower temperatures and in the presence of adsorbed CO the (5 × 1) structure can be locally lifted to the (1 × 1) structure. After CO desorption the (5 × 1) structure was fully recovered.

■ ASSOCIATED CONTENT

Supporting Information

The Supporting Information is available free of charge on the ACS Publications website at DOI: 10.1021/acs.jpcc.5b12494.

C 1s X-ray photoelectron spectra conforming the absence of carbon on the surface; O 1s XPS spectra showing the removal of oxygen from the Ir(2 × 1)-O surface; discussion of LEED structures (PDF)

■ AUTHOR INFORMATION

Corresponding Author

*E-mail: christoph.rameshan@tuwien.ac.at.

Present Address

§BASF Catalysts Germany GmbH, Grosser Drakenburger Strasse 133, 31582 Nienburg, Germany. Hao.li@basf.com.

Notes

The authors declare no competing financial interest.

■ ACKNOWLEDGMENTS

This work was supported by the Austrian Science Fund (FWF) through the international DACH program I 1041-N28 (COMCAT) and through project SFB FOXSI (F4502-N16).

■ REFERENCES

(1) Titmuss, S.; Wander, A.; King, D. A. Reconstruction of Clean and Adsorbate-Covered Metal Surfaces. *Chem. Rev.* **1996**, *96*, 1291−1305.

(2) Lehwald, S.; Chen, J. G.; Kisters, G.; Preuss, E.; Ibach, H. Surface-Phonon Dispersion Investigation of the (1 × 1) - (5 × 1) Reconstruction of the Ir(100) Surface. *Phys. Rev. B: Condens. Matter Mater. Phys.* **1991**, *43*, 3920−3927.

(3) Hohenberg, P.; Kohn, W. Inhomogeneous Electron Gas. *Phys. Rev.* **1964**, *136*, B864−B871.

DOI: 10.1021/acs.jpcc.5b12494
J. Phys. Chem. C 2016, 120, 10838−10848

(4) Ge, Q.; King, D. A.; Marzari, N.; Payne, M. C. First Principles Calculation of the Energy and Structure of Two Solid Surface Phases on Ir{100}. *Surf. Sci.* **1998**, *418*, 529−535.
(5) Hammer, L.; Meier, W.; Klein, A.; Landfried, P.; Schmidt, A.; Heinz, K. Hydrogen-Induced Self-Organized Nanostructuring of the Ir(100) Surface. *Phys. Rev. Lett.* **2003**, *91*, 156101.
(6) Sales, B. C.; Turner, J. E.; Maple, M. B. Oscillatory Oxidation of CO over Pt, Pd and Ir Catalysts - Theory. *Surf. Sci.* **1982**, *114*, 381−394.
(7) Marino, F.; Descorme, C.; Duprez, D. Noble Metal Catalysts for the Preferential Oxidation of Carbon Monoxide in the Presence of Hydrogen (PROX). *Appl. Catal., B* **2004**, *54*, 59−66.
(8) Broden, G.; Rhodin, T. N. Chemisorption of CO on Ir(100) Studied by Photoemission. *Solid State Commun.* **1976**, *18*, 105−109.
(9) Martin, R.; Gardner, P.; Nalezinski, R.; Tushaus, M.; Bradshaw, A. M. The C-O Stretch as a Probe of Adsorbate-Induced Structural-Changes on Surfaces - Ir(100)-CO. *J. Electron Spectrosc. Relat. Phenom.* **1993**, *64-65*, 619−626.
(10) Kisters, G.; Chen, J. G.; Lehwald, S.; Ibach, H. Adsorption of CO on the Unreconstructed and Reconstructed Ir(100) Surface. *Surf. Sci.* **1991**, *245*, 65−71.
(11) Chen, W. H.; Ermanoski, I.; Jacob, T.; Madey, T. E. Structure Sensitivity in the Oxidation of CO on Ir Surfaces. *Langmuir* **2006**, *22*, 3166−3173.
(12) Lauterbach, J.; Boyle, R. W.; Schick, M.; Mitchell, W. J.; Meng, B.; Weinberg, W. H. The Adsorption of CO on Ir(111) Investigated with FT-IRAS. *Surf. Sci.* **1996**, *350*, 32−44.
(13) Minguzzi, A.; Lugaresi, O.; Achilli, E.; Locatelli, C.; Vertova, A.; Ghigna, P.; Rondinini, S. Observing the Oxidation State Turnover in Heterogeneous Iridium-Based Water Oxidation Catalysts. *Chem. Sci.* **2014**, *5*, 3591−3597.
(14) Coraux, J.; N'Diaye, A. T.; Busse, C.; Michely, T. Structural Coherency of Graphene on Ir(111). *Nano Lett.* **2008**, *8*, 565−570.
(15) Meyer, W.; Biedermann, K.; Gubo, M.; Hammer, L.; Heinz, K. Surface Structure of Polar Co3O4(111) Films Grown Epitaxially on Ir(100)-(1 × 1). *J. Phys.: Condens. Matter* **2008**, *20*, 265011.
(16) Freund, H.-J.; Meijer, G.; Scheffler, M.; Schlogl, R.; Wolf, M. CO Oxidation as a Prototypical Reaction for Heterogeneous Processes. *Angew. Chem., Int. Ed.* **2011**, *50*, 10064−10094.
(17) Giovanardi, C.; Hammer, L.; Heinz, K. Ultrathin Cobalt Oxide Films on Ir(100)-(1 × 1). *Phys. Rev. B: Condens. Matter Mater. Phys.* **2006**, *74*, 125429.
(18) Mehl, S.; Ferstl, P.; Schuler, M.; Toghan, A.; Brummel, O.; Hammer, L.; Schneider, M. A.; Libuda, J. Thermal Evolution of Cobalt Deposits on Co3O4(111): Atomically Dispersed Cobalt, Two-Dimensional CoO Islands, and Metallic Co Nanoparticles. *Phys. Chem. Chem. Phys.* **2015**, *17*, 23538−23546.
(19) Ferstl, P.; Mehl, S.; Arman, M. A.; Schuler, M.; Toghan, A.; Laszlo, B.; Lykhach, Y.; Brummel, O.; Lundgren, E.; Knudsen, J.; et al. Adsorption and Activation of CO on Co3O4(111) Thin Films. *J. Phys. Chem. C* **2015**, *119*, 16688−16699.
(20) Rupprechter, G. A Surface Science Approach to Ambient Pressure Catalytic Reactions. *Catal. Today* **2007**, *126*, 3−17.
(21) Rupprechter, G. Sum Frequency Generation and Polarization-Modulation Infrared Reflection Absorption Spectroscopy of Functioning Model Catalysts from Ultrahigh Vacuum to Ambient Pressure. *Adv. Catal.* **2007**, *51*, 133−263.
(22) Rupprechter, G. Surface Vibrational Spectroscopy from Ultrahigh Vacuum to Atmospheric Pressure: Adsorption and Reactions on Single Crystals and Nanoparticle Model Catalysts Monitored by Sum Frequency Generation Spectroscopy. *Phys. Chem. Chem. Phys.* **2001**, *3*, 4621−4632.
(23) Rupprechter, G.; Dellwig, T.; Unterhalt, H.; Freund, H. J. High-Pressure Carbon Monoxide Adsorption on Pt(111) Revisited: A Sum Frequency Generation Study. *J. Phys. Chem. B* **2001**, *105*, 3797−3802.
(24) Heinz, K.; Hammer, L. Nanostructure Formation on Ir(100). *Prog. Surf. Sci.* **2009**, *84*, 2−17.
(25) Lerotholi, T. J.; Held, G.; King, D. A. Phase Mixing and Phase Separation Accompanying the Catalytic Oxidation of CO on Ir{100}. *Surf. Sci.* **2007**, *601*, 1285−1295.
(26) Hollins, P. Infrared Reflection−Absorption Spectroscopy. In *Encyclopedia of Analytical Chemistry*; John Wiley & Sons, 2000.
(27) VanHove, M. A.; Weinberg, W. H.; Chan, C. M. Low-Energy Electron Diffraction: Experiment. In *Theory and Surface Structure Determination*; Springer: Berlin Heidelberg, 2012.
(28) Scheffler, M. Infuence of Lateral Interactions on the Vibrational-Spectrum of Adsorbed CO. *Surf. Sci.* **1979**, *81*, 562−570.
(29) Persson, B. N. J.; Ryberg, R. Vibrational Interaction Between Molecules Adsorbed on a Metal-Surface - The Dipole-Dipole Interaction. *Phys. Rev. B: Condens. Matter Mater. Phys.* **1981**, *24*, 6954−6970.
(30) Schmidt, A.; Meier, W.; Hammer, L.; Heinz, K. Deep-Going Reconstruction of Ir(100)-5 × 1. *J. Phys.: Condens. Matter* **2002**, *14*, 12353−12365.
(31) Deshlahra, P.; Conway, J.; Wolf, E. E.; Schneider, W. F. Influence of Dipole-Dipole Interactions on Coverage-Dependent Adsorption: CO and NO on Pt(111). *Langmuir* **2012**, *28*, 8408−8417.
(32) Titmuss, S.; Johnson, K.; Ge, Q.; King, D. A. Structure, Bonding, and Anharmonic Librational Motion of CO on Ir{100}. *J. Chem. Phys.* **2002**, *116*, 8097−8105.
(33) Kildemo, M.; Ramsvik, T.; Raaen, S. Investigation of the La-Rh(100) Surface Alloy. *Surf. Sci.* **2001**, *490*, 1−12.
(34) Oura, K.; Lifshits, V. G.; Saranin, A.; Zotov, A. V.; Katayama, M. *Surface Science: An Introduction*; Springer: Berlin Heidelberg, 2013; p 314.

DOI: 10.1021/acs.jpcc.5b12494
J. Phys. Chem. C 2016, 120, 10838−10848